

This article was downloaded by:

On: 22 January 2011

Access details: *Access Details: Free Access*

Publisher *Taylor & Francis*

Informa Ltd Registered in England and Wales Registered Number: 1072954 Registered office: Mortimer House, 37-41 Mortimer Street, London W1T 3JH, UK



The Journal of Adhesion

Publication details, including instructions for authors and subscription information:

<http://www.informaworld.com/smpp/title~content=t713453635>

Finite element analysis of adhesive joints in four-point bending load

A. Ozel^a; F. Kadioglu^a; S. Sen^a; R. Sadeler^a

^a Engineering Faculty, Mechanical Engineering Department, Ataturk University, Erzurum, Turkey

Online publication date: 08 September 2010

To cite this Article Ozel, A. , Kadioglu, F. , Sen, S. and Sadeler, R.(2010) 'Finite element analysis of adhesive joints in four-point bending load', *The Journal of Adhesion*, 79: 7, 683 – 697

To link to this Article: DOI: 10.1080/00218460309579

URL: <http://dx.doi.org/10.1080/00218460309579>

PLEASE SCROLL DOWN FOR ARTICLE

Full terms and conditions of use: <http://www.informaworld.com/terms-and-conditions-of-access.pdf>

This article may be used for research, teaching and private study purposes. Any substantial or systematic reproduction, re-distribution, re-selling, loan or sub-licensing, systematic supply or distribution in any form to anyone is expressly forbidden.

The publisher does not give any warranty express or implied or make any representation that the contents will be complete or accurate or up to date. The accuracy of any instructions, formulae and drug doses should be independently verified with primary sources. The publisher shall not be liable for any loss, actions, claims, proceedings, demand or costs or damages whatsoever or howsoever caused arising directly or indirectly in connection with or arising out of the use of this material.

FINITE ELEMENT ANALYSIS OF ADHESIVE JOINTS IN FOUR-POINT BENDING LOAD

A. Ozel
F. Kadioglu
S. Sen
R. Sadeler

Engineering Faculty, Mechanical Engineering Department,
Ataturk University, Erzurum, Turkey

Nonlinear finite element analysis (FEA) was applied to the adhesively bonded Single Lap Joint (SLJ) in bending load. Two adhesives, one stiff and one flexible, with very different mechanical behaviors, and hard steel as adherend with four different thicknesses, were analyzed for the joint configuration. For comparison, experimental work was also undertaken.

It was shown that adherend thickness played an important part in the joint performance; while the stiff adhesive gave stronger joint strength when using thick adherends, the opposite was the case for the flexible adhesive when using thin adherends. These results were related to the mechanical behaviors of the adhesives used. It was shown that the results from the FEA and the experimental works were in a good agreement.

Keywords: Adhesives; Nonlinear analysis; Single lap joint; Bending test

INTRODUCTION

Adhesive bonding is extensively used to join both metallic and composite aircraft structural components, and as a method for repairing damaged structural components. The design process requires an accurate knowledge of stress-strain behavior of the structural adhesive [1], and there are several test methods for this purpose [2].

Received 6 July 2002; in final form 14 December 2002.

Address correspondence to Ferhat Kadioglu, University of Ataturk, Department of Mechanical Engineering, 25240 Erzurum, Turkey. E-mail: ferhat.kadioglu@mailcity.com

The single lap joint (SLJ) configuration is one form of adhesive joint that receives much attention from engineers due to its simplicity and similarity to working conditions. As explained by some researchers [3–5], the joint is not under pure shear when the tensile load is applied. It was shown that the peel and shear stresses in the adhesive are not uniform along the overlap length, resulting in a complex behavior of the joint under loading. In order to predict the joint strength, over the past 50 years there have been numerous studies conducted and information collected on the stress analysis of adhesively bonded single-lap joints. The pioneering work by Volkersen [4] published the first known stress analysis by considering only the stresses arising from differential shearing. Goland and Reissner [5] extended this analysis by calculating the stresses due to both bending and differential shearing, thereby obtaining expressions for the shear and transverse tensile stresses in the adhesive layer. In most cases, the SLJ configuration in tensile load was analysed for better predictions [6–10]. Such joints can experience a bending load under working conditions as well, and there are few researchers investigating the effects of the load. For example, Lui *et al.* [11] studied the stress distributions of the joint subjected to external bending moment, using one type of adhesive and two types of adherends. In the numerical calculations, the effects of the ratio of the Young's moduli of adherends, the adherend thickness ratio and the adherend length ratio between dissimilar adherends on the stress distributions at the interfaces were examined. From this work, it was found that the joint strength increased as Young's modulus of the adherends and adherend thickness increased, while the effect of the adherend lengths on the joint strength was small. The SLJ of similar adherends under bending load was also investigated by Lui and Sawa [12] and by Harada *et al.* [13]. In establishing an optimal design of adhesive joints, it is necessary to focus on the behavior of different adhesives in the joint configuration when subjected to external bending moments.

The aim of this paper is to assess the performance of two different adhesives in the single lap joint, and to analyse the stress distribution in the joint in bending mode for better understanding of the failure mechanisms, using nonlinear finite element analysis (FEA). In the analysis, consideration was given to the adherends used as well as the adhesive layer, as some critical points on the adherends were expected. Also, the FEA results were compared with experimental ones.

FINITE ELEMENT ANALYSIS

For the investigation of stress distributions in the SLJ in four-point bending load, a nonlinear finite element method was applied, using the ANSYS 5.7.1 Package. Plane 42 was chosen as an element type, which is used for 2-D modeling of solid structures. The element can be used either as a plane element (plane stress or plane strain) or as an axisymmetric element. The element is defined by four nodes having two degrees of freedom at each node: translations in the nodal x and y directions. The element has plasticity, creep, swelling, stress stiffening, large deflection, and large strain capabilities [14]. The number of elements was changed for every thickness of adherend and small elements were used for critical regions. Boundary conditions for the joints are shown in Figure 1.

The SLJ under bending loads has been shown to experience multi-axial stress distributions, especially around the region of the adhesive layer [11]. In this study, the stresses at this region were indicated by using the Von Mises stress-criterion, which allows the multi-axial stresses to be transferred into uniaxial stresses. Accordingly, when the Von Mises stresses at the critical zones, such as at the ends of the overlap, reached the ultimate uni-axial stresses of the materials used, shown in Figures 2–4, it was assumed that the failure of the joints took place. Then the assumed failure stresses were compared with the experimental failure of the joints.

Two different types of adhesives were used in the analysis in order to assess the effect of the material behaviors on the performance of the joints. Figure 2 shows the tensile stress-strain behavior of a very ductile adhesive, 9245 SBT produced by 3M (St. Paul, Minnesota, USA) while Figure 3 is a tensile stress-strain behavior of a modern structural epoxy adhesive, AV119, produced by Ciba (Ciba Polymers,

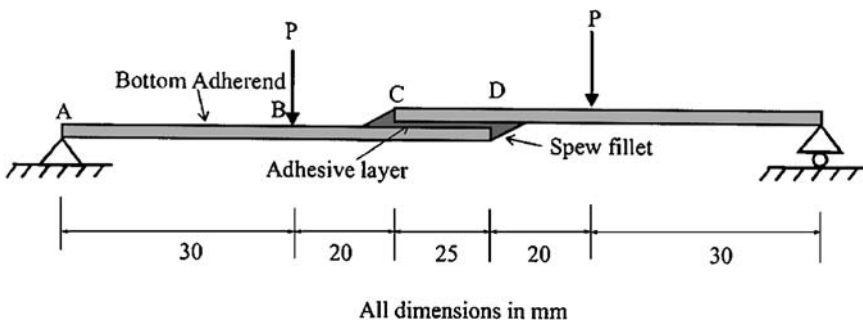


FIGURE 1 Boundary conditions for SLJ configurations.

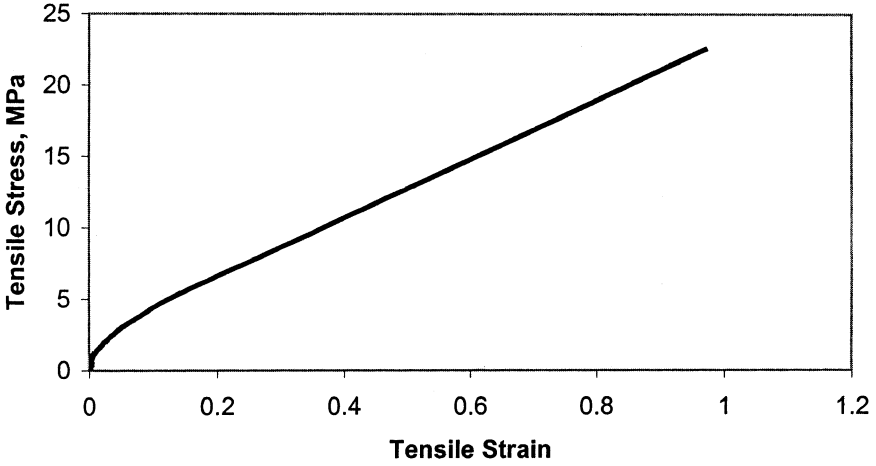


FIGURE 2 Tensile stress-strain behavior of SBT adhesive.

Duxford, Cambridge, UK). Hard steel was used as adherend to avoid plastic deformation as explained elsewhere [15]. The tensile behavior of the adherend is shown in Figure 4. For more details of mechanical behavior of the materials, more information can be obtained from Kadioglu [2].

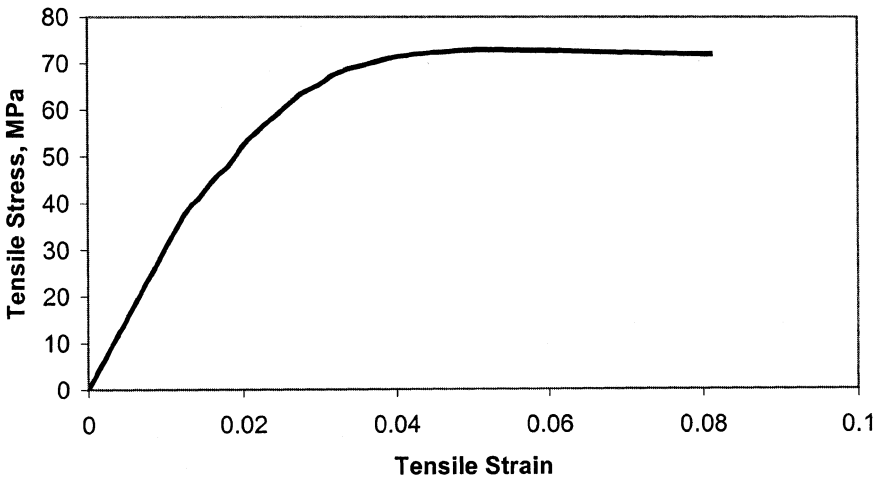


FIGURE 3 Tensile stress-strain behavior of AV119 adhesive.

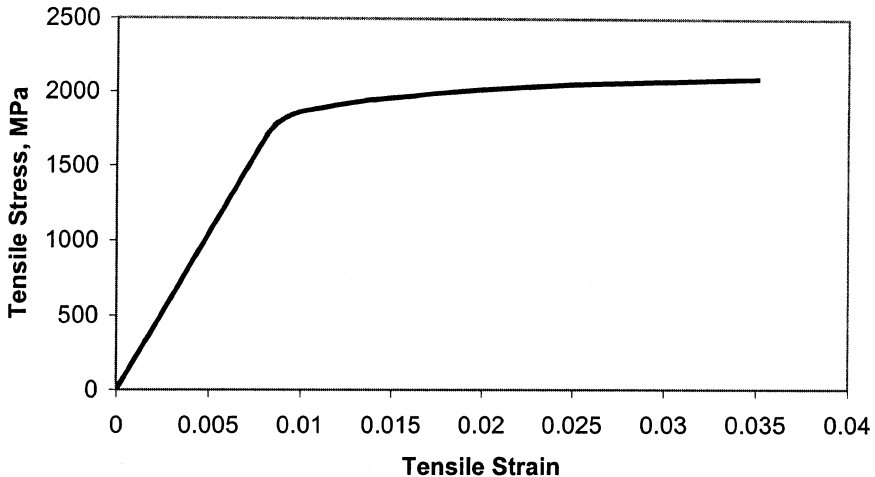


FIGURE 4 Tensile stress-strain behavior of hard steel.

It should be pointed out that some spacers were used to control the adhesive thickness and spew fillets formed from the excess liquid adhesive which was squeezed out during fabrication of the joints. Since the AV119 adhesive was in its liquid state during fabrication of the AV119 joints, the spew fillets were formed at the ends of the overlap, which was not the case for the SBT joints, where SBT was in its solid state during manufacture. Correspondingly, when the joints were modeled for the FEA, the spew fillets were included in the model only for the AV119 joints.

EXPERIMENTAL

For the joining process, the surface portion of the adherend to be bonded was cleaned with acetone, and then grit-blasted, and then acetone was used again to clean the adherends just before the application of the adhesives. The cure processes for the SBT and AV119 joints were 45 min at 140°C and 60 min at 120°C, respectively. After the cure of the joints, they were allowed to cool and then they were removed from the jig in which they were produced.

The four-point bending rig, which is described in detail elsewhere [16], was mounted on the Zwick Testing Machine (Zwick Testing Machines, Herefordshire, UK) to conduct the test. To achieve a true representation of pure bending, all four point loads had to contact the surface of the horizontal single lap joint simultaneously. This was achieved by positioning some specially prepared spacers.

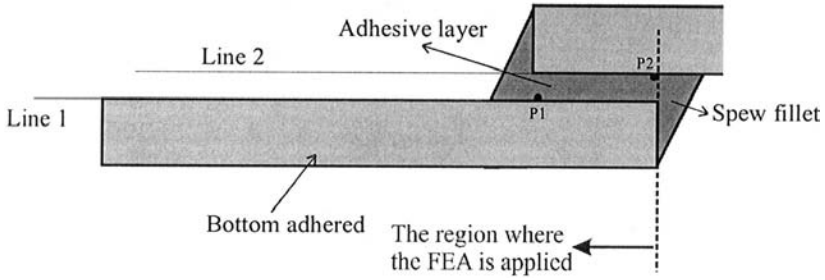


FIGURE 5 The part of SLJ where the FEA is applied.

RESULTS

Finite Element Analysis

It should be noted that the bottom adherends on the left side of the joints were taken into consideration for FEA. Also, the upper line of the adherends but bottom line of the adhesive was analyzed when producing FE results (see Figure 5). It should be pointed out that the stress distributions in line 1 are different from those of line 2; Figures 6 and 7 show the von Mises (seqv) stress distributions of SBT and AV119, respectively, across the line 1 and line 2. From the figure it is

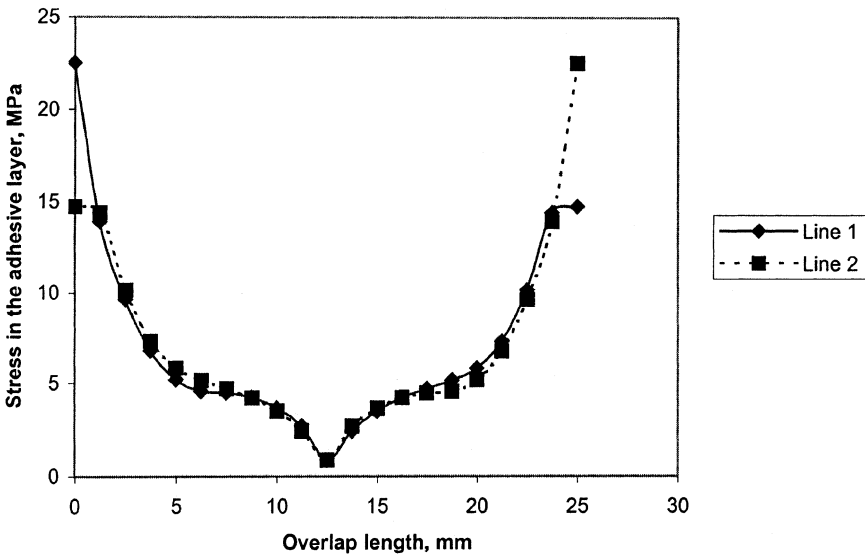


FIGURE 6 The von Mises stresses in the SBT adhesive layer.

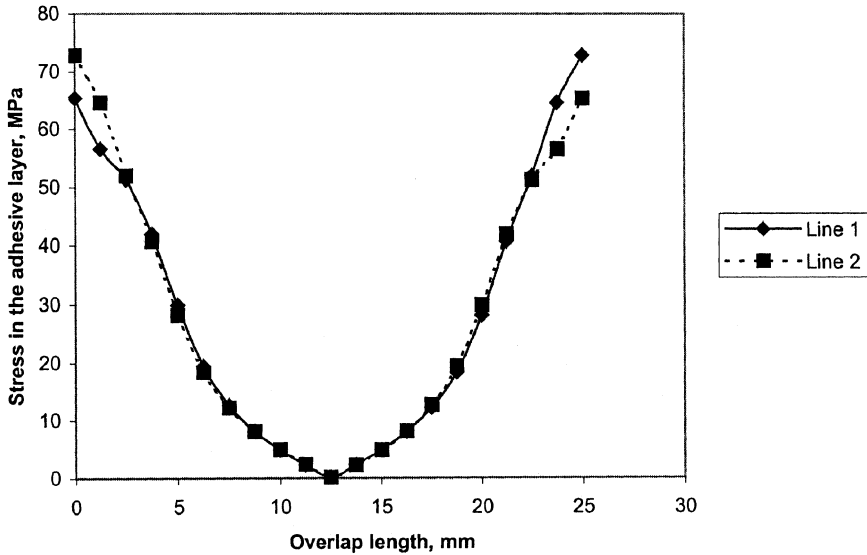


FIGURE 7 The von Mises stresses in the AV119 adhesive layer.

seen that the von Mises stresses of SBT have their peak values at point P1 for line 1 and at point P2 for line 2. These results are opposite for AV119, which can be attributed to the spew fillet effects leading to stress relief at the ends of the overlap (see Figure 5). Similar discrepancies at the overlap ends should also be attributed to the fillet effects, which is only the case for the AV119 joints (*i.e.*, as already mentioned in the above section, “Finite Element Analysis,” the AV119 joints were modeled including the spew fillet at the end of the overlap, which was not the case for the SBT joints. This leads to different stress distributions of AV119 and SBT across line 1 and line 2).

Relatively more effective stresses in the adherend and adhesive layer were considered to be taken into account when producing FE results; Figures 8 and 9 show the von Mises stresses (σ_{eq}), shear stresses (τ_{sxy}), stresses in the x direction (σ_x) and stresses in the y direction (σ_y) in the adherend and in the adhesive layer, respectively, for the SBT joints.

It can be seen from Figure 8 that τ_{sxy} and σ_y stresses are very low compared with σ_x and σ_{eq} so they can be ignored when analyzing the adherends. Also, since σ_x and σ_{eq} stresses produce nearly the same results, but with the opposite signs, only the von Mises stresses will be considered for the upcoming results in the adherends. Figure 9 shows that τ_{sxy} stresses in the adhesive layer are less effective than the

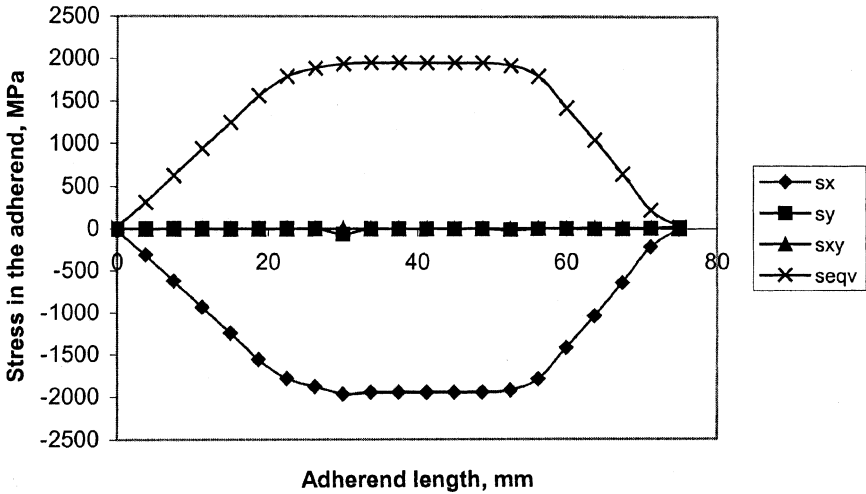


FIGURE 8 Stress distributions in the bottom adherends of the SBT joints.

others (s_x , s_y , and s_{eqv}), therefore, s_{xy} stresses will not be taken into consideration for upcoming FE results.

Figures 10, 11 and Figure 12 show the s_x , s_y , and s_{eqv} stress distributions, respectively, in the SBT adhesive layer. It is interesting to note that the stress concentrations in the adhesive layer are relatively

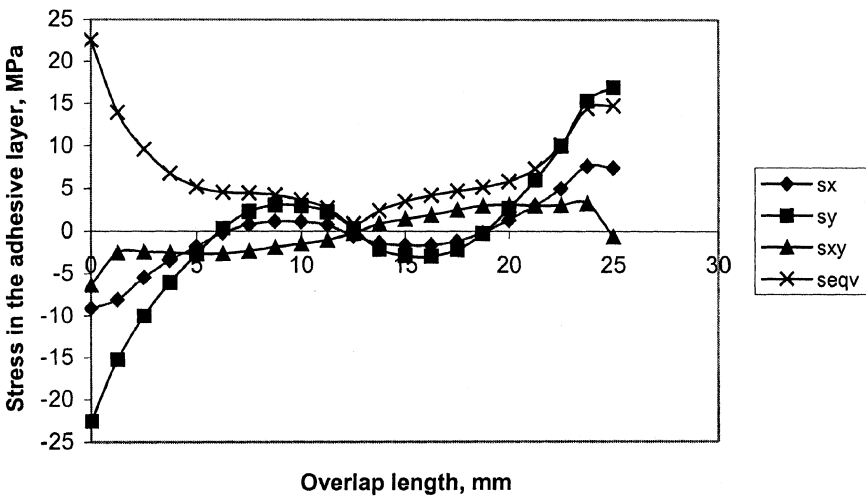


FIGURE 9 Stress distributions in the SBT adhesive layer.

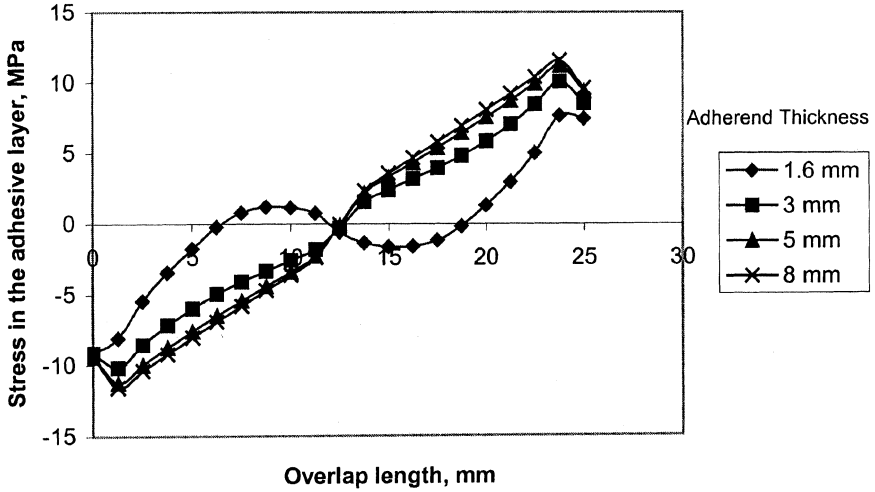


FIGURE 10 SX stress distributions in the SBT adhesive layer.

small in the zone near the middle of the overlap, especially for the thin adherend (1.6 mm), but they are very high at the ends of the overlap. For the thicker adherends, a linear increase in the stress concentrations is observed from the middle to the ends of the overlap. It can be

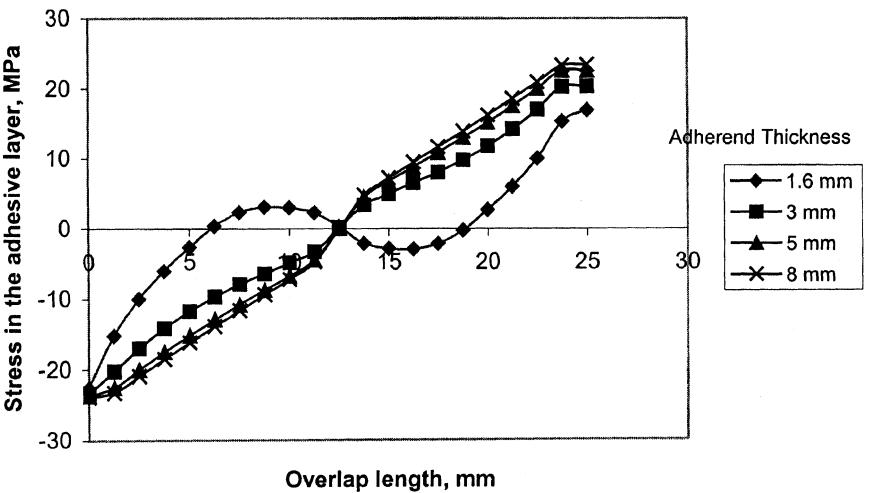


FIGURE 11 SY stress distributions in the SBT adhesive layer.

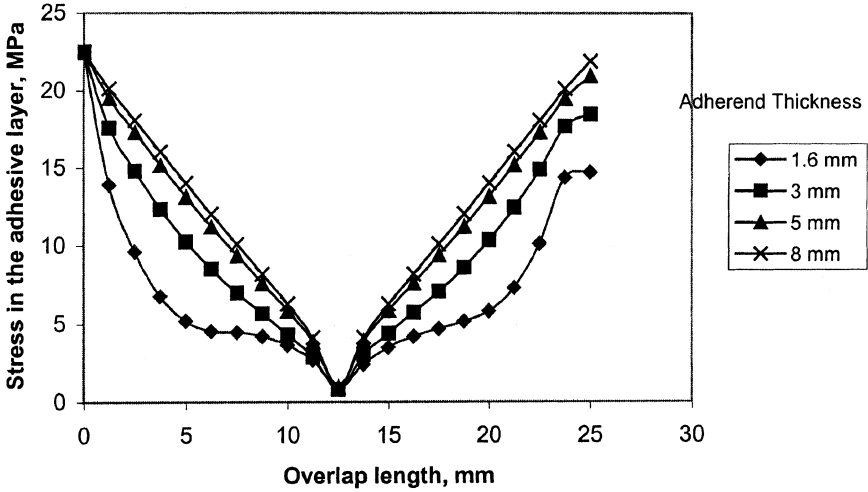


FIGURE 12 Von Mises stress distributions in the SBT adhesive layer.

seen from the figures that σ_y and σ_{xy} stresses (see Figures 11 and 12) are more effective than the σ_x stresses (see Figure 10).

Figure 13 shows the stress distributions in the bottom adherends of the SBT joints, on the leftside hand (AD line, see Figure 1). It is seen that there is a nearly linear increase of stresses in the adherends up to

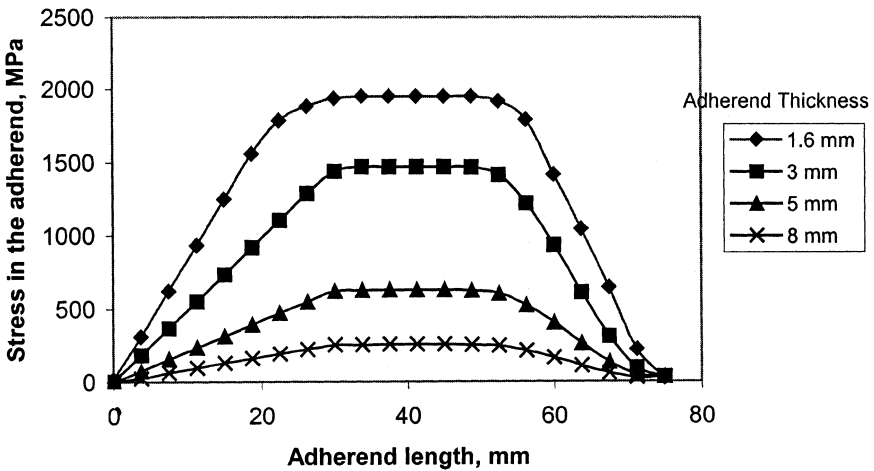


FIGURE 13 Von Mises stress distributions in the bottom adherends of the SBT joints.

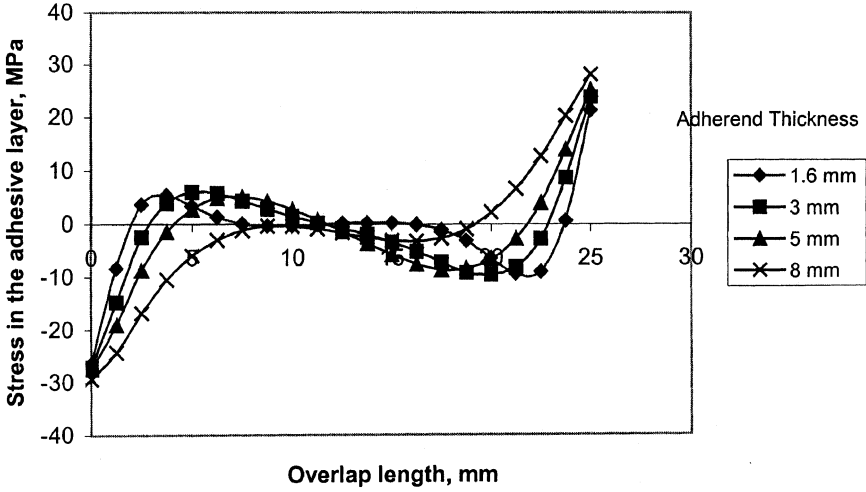


FIGURE 14 SX stress distributions in the AV119 adhesive layer.

the applied load and then a constant stress distribution is observed from the applied load to the point where the adhesive layer begins (line BC, see Figure 1). It should be pointed out that the adherend with the thickness of 1.6 mm is quite stressed and it is likely to fail before the failure of the ductile adhesive (SBT). To have a clear idea for this,

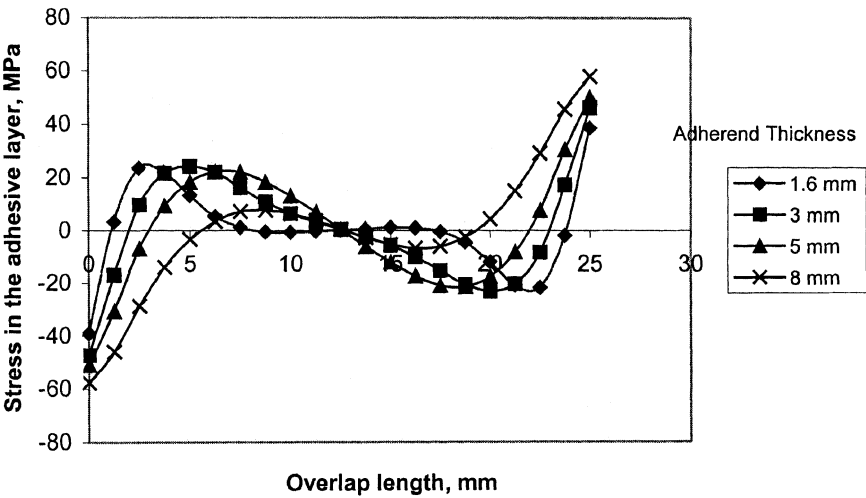


FIGURE 15 SY stress distributions in the AV119 adhesive layer.

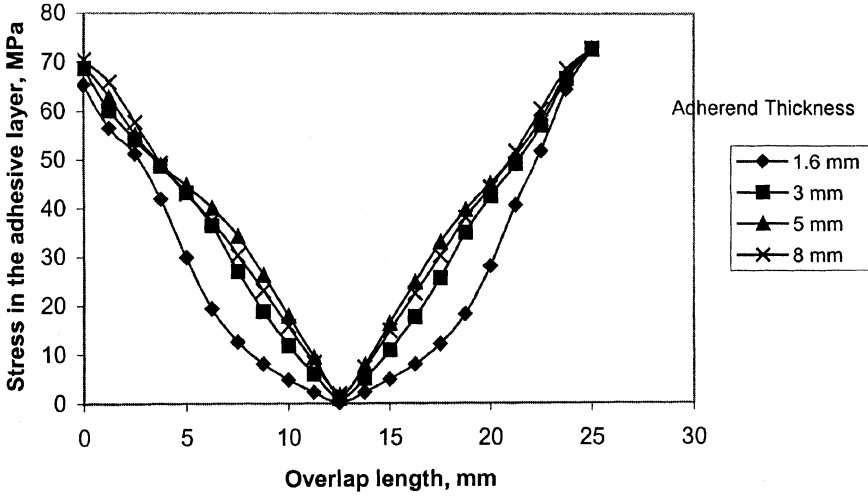


FIGURE 16 Von Mises stress distributions in the AV119 adhesive layer.

Figures 4 and 13 should be studied very carefully; from Figure 4 it is seen that the adherend has a maximum tensile stress of about 2000 MPa, which is very close to the peak value occurring in the adherend with 1.6 mm thickness.

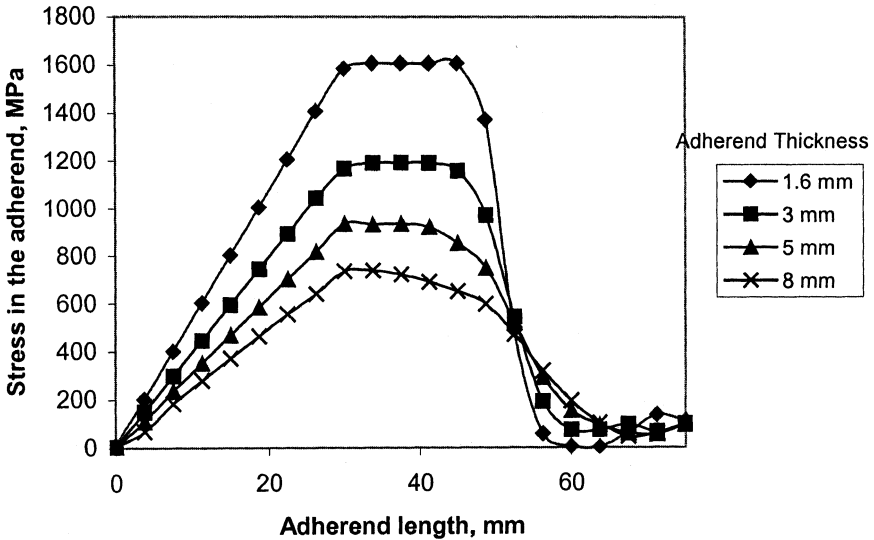


FIGURE 17 Stress distributions in the bottom adherends of the AV119 joints.

TABLE 1 A Comparison of Results from the FEA and Experiments for the SBT and AV119 Joints

Adherend thickness, mm	Predicted results (PR), N	Experimental results (ER), N	% difference between PR and ER	Joint names
1.6	1775	1600	10.9	SBT joint
	1140	1030	10.6	AV119 joint
3	3675	3036	21.0	SBT joint
	2977.5	2527	17.8	AV119 joint
8	4585	5670	23.6	SBT joint
	13200	11620	13.5	AV119 joint

Figures 14–16 show the s_x , s_y , and s_{eq} stress distributions in the AV119 layer, which are similar to the SBT layer. Stress concentrations are very high at the ends of the overlap but relatively small around the middle. The stress distributions in the bottom adherends of AV119 joints are shown in Figure 17. It is seen that all the results are similar to the adherends from the SBT joints, except the one with 1.6 mm thickness; it is clear that this adherend is not as stressed as that of the SBT joint, which implies the SBT joints are stronger than the AV119 joints for the adherends with 1.6 mm thickness. The failure predictions of the SBT joints and AV119 joints are shown in Table 1. It is seen that SBT joints are stronger than the AV119 joints for the thin adherends (1.6 mm and 3 mm), while the opposite is the case for the thick adherends.

Experimental Results

All the specimens having an adhesive layer thickness of 0.4 mm were tested at constant temperature and relative humidity, 23°C and 50%, respectively, and the crosshead speed was 5 mm/min. Five joints were tested for every adherend thickness (1.6 mm, 3 mm, and 8 mm) for two different adhesive materials (SBT and AV119).

When SBT joints of 1.6 mm adherend thickness were tested in the four-point bend test, high deflections of joints in the y direction were experienced, which caused the failure to take place in the adherends as well as in the joints. There were four possible critical points on the specimen; two were at the ends of the overlap and the other two were at the points where the loads were applied. The SBT joints with 3 mm adherends gave smaller deflections but higher failure loads. All the failures occurred in the overlap region without breaking the adherends. The failure of the SBT joints with 8 mm adherend thickness was found to be similar to those with 3 mm adherends. Again, smaller joint deflections but increased failure loads were experienced. All the AV119

joints failed in the overlap region without breaking the adherends, which was similar to the SBT joints with 3 mm and 8 mm adherend thicknesses. In general, it was seen that the initial failure of the joints commenced at the ends of the overlap. A comparison of results from both experiments and FEA is shown in Table 1. It is seen that they are in good agreement.

DISCUSSION

In general, stress concentrations in the adhesive layer are very high at the ends of the overlap, which is assumed to be the cause of the initial failure of the joints. It is important to note that as the adherend thickness increases the value of stresses also increases towards the midpoint of the overlap, which implies that the applied load can be carried by the relatively larger area of the overlap. This is especially the case for the joints with the ductile adhesive, SBT, shown in Figures 10 and 11. It should be pointed out that the load transfer capacity of SBT is better than that of AV119 for thin adherends due to its high strain to failure, which enables the applied load to be carried by a larger area of the overlap and the joint to be stronger (see Table 1). Also, the flexible properties of SBT contribute to the stress relief at the ends of the overlap, reducing the stress concentrations shown in Figure 10. However, the concentrations at the overlap ends are considerably higher for the AV119 joints compared with the SBT joints. This is thought to be due to the mechanical behavior of the stiff adhesive, AV119, shown in Figure 3, which shows a relatively small strain to failure compared with Figure 2. As shown in Figure 14 and Figure 15, the AV119 joints with thin adherends (1.6 mm and 3 mm) experience such high concentrations at the ends that the stress distributions around the middle of the overlap have very low values, which leads to the joints carrying the applied loads only at the ends of the overlap. This limits the load transfer capacity of AV119 and reduces the joint performance.

Results from FEA and experiments showed that the maximum strength of the joints are in agreement, which is shown in Table 1. It can be seen from the table that when using the adherends with thicknesses of 1.6 mm and 3 mm, the strength of the AV119 joints are lower than those of SBT joints. However, the opposite is the case for the thick adherends.

As explained earlier, not all the failures of the SBT joints of 1.6 mm adherend thickness happened in the adhesive layer. Towards the end of the test, some noises were emitted and then the failure took place. It seemed that some adherends had been broken near the loading points.

This can also be seen from the FEA results, which show that the SBT joints with 1.6 mm adherend thickness have very high stress concentrations (see Figure 13). All the failures of the AV119 joints happened in the adhesive layer.

CONCLUSIONS

It was shown that the adherend thickness played an important part in the performance of the single lap joint in bending load. The stiff adhesive was stronger than the flexible adhesive in joints with the thick adherends; however, the opposite was the case for the joints with the thin adherends, which was related to the mechanical behaviors of the adhesives used. It was shown that results from the FEA and the experimental works were comparable.

REFERENCES

- [1] Chiu, W. K. and Jones, R., *Int. J. Adhesion and Adhesives*, **12**(3), 219–225 (1992).
- [2] Kadioglu, F., Quasi-Static and Dynamic Behavior of a Structural Pressure-Sensitive Adhesive, Ph.D. Thesis, Mechanical Engineering, University of Bristol, Bristol, UK (2000).
- [3] Adams, R. D. and Peppiat, N. A., *J. Strain Analysis*, **9**(3), 185–196 (1974).
- [4] Volkersen, O., Die Nietkraftverteilung in Zugbeanspruchten Nietverbindungen mit Konstanten Laschquerschnitten, *15 Luftfahrtforschung* **15**, 41–47 (1938).
- [5] Goland, M. and Reissner, E., *J. Appl. Mech. Trans. ASME*, **66**, A17–A27 (1944).
- [6] Hart-Smith, L. J., *Adhesive Bonded Single Lap Joints*, NASA Report CR-112236, CR-112237, Langley Research Center, Hampton, Virginia, (1973).
- [7] Tsai, M. Y. and Morton, J., *Int. J. Solid Structures*, **31**(18), 2537–2563 (1994).
- [8] Tsai, M. Y., Oplinger, D. W. and Morton, J., *Int. J. Solid Structures*, **35**(12), 1163–1185 (1998).
- [9] Lang, T. P. and Mallick, P. K., *Int. J. Adhesion Adhesives*, **18**, 167–177 (1998).
- [10] Harris, J. A., Non Linear Analysis and Testing of Adhesive Joints Under Impact and Quasi-Static loading, Ph.D. Thesis, Mechanical Engineering, University of Bristol, Bristol, UK (1983).
- [11] Lui, J., Sawa, T. and Toratani, H., *J. Adhesion*, **69**, 263–291 (1999).
- [12] Lui, J. and Sawa, T., *J. Adhesion Sci. Technol.*, **12**, 795–812 (1998).
- [13] Harada, K., Hamada, H. and Maekawa, Z., *J. Adhesion Sci. Technol.*, **10**, 1089–1104 (1996).
- [14] ANSYS, The General Purpose Finite Element Software, Swanson Analysis Systems, Inc., Houston, Texas.
- [15] Karachalios, V. F., Stress and Failure Analysis of Adhesively Bonded Single Lap Joint, Ph.D. Thesis, Mechanical Engineering, University of Bristol, Bristol, UK, (1999).
- [16] Kadioglu, F., Ozel, A. and Adams, R. D., “The strength in the weakness” to be published in the *Journal of Advanced Materials*.